



Tetrathiafulvalene hydrazone an efficient precursor of various chelating electroactive ligands

Michel Guerro^a, To Uyen Dam^a, Saleha Bakhta^{a,b,c}, Bellara Kolli^b, Thierry Roisnel^a, Dominique Lorcy^{a,*}

^a Sciences Chimiques de Rennes (SCR), UMR 6226 CNRS-Université de Rennes 1, Campus de Beaulieu, 263, Avenue du Général Leclerc, Bât 10A, 35042 Rennes cedex, France

^b Laboratoire de chimie organique Université des Sciences et de la Technologie "HouariBoumediène"(USTHB), 16111 Alger, Algeria

^c Centre de Recherche Scientifique et Technique en Analyse Physico-Chimiques (CRAPC) BP 248, Alger RP16004, Alger, Algeria

ARTICLE INFO

Article history:

Received 15 February 2011

Received in revised form 15 March 2011

Accepted 16 March 2011

Available online 23 March 2011

Keywords:

Tetrathiafulvalene

Chelating ligands

Redox behaviour

Molybdenum

Boron difluoride

ABSTRACT

Novel bidentate electroactive ligands containing one or two tetrathiafulvalene (TTF) cores as redox active unit have been synthesized thanks to the condensation of various carbonyl derivatives with TTF hydrazone. The electron donating ability of these redox active ligands determined by cyclic voltammetry is described together with the investigations of their molecular structures by X-ray diffraction studies. The chelating ability of these ligands has been exemplified through the coordination to molybdenum carbonyl fragment or the complexation to difluoroboron moiety.

© 2011 Elsevier Ltd. All rights reserved.

1. Introduction

An easy route for the synthesis of electroactive ligands, such as tetrathiafulvalene-based ligands consists in the grafting of a coordination function on the preformed tetrathiafulvalene (TTF) core.¹ For that purpose, an anchoring group is first introduced on the TTF core, and subsequent reaction of this group with a coordination function allows the synthesis of TTF ligands. Accordingly, various TTF ligands have been prepared and coordinated to different metallic fragments in order to build hybrid organic–inorganic building blocks.^{1,2} Among the various anchoring groups used for that purpose, we recently demonstrated the potentialities of hydrazino-TTF as it condensed with either pyridine carboxaldehyde or salicylaldehyde to form (N,O) and (N,N) bidentate TTF-based ligands thanks to the formation of the azino linker (molecules **A**, Fig. 1).³ Using this strategy, we prepared TTFs that contain structural moieties for metal chelation as the azino linker participates in the coordinating activity.

This work has been extended here to the synthesis of novel (N,S), and (N,N) bidentate ligands thanks to the condensation of hydrazino-TTF with various aldehydes bearing a heterocycle, such as thiophene and pyrrole (molecules **B**, Fig. 2). We also investigated

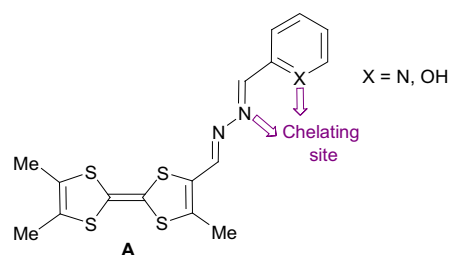


Fig. 1. Bidentate (N,O) and (N,N) TTF-based ligands.

the synthesis of (N,O) bidentate Nacac-type ligands, such as TTF substituted with a β -enaminoketone chelating group (molecules **C**, Fig. 2). Indeed, β -enaminoketonato ligand⁴ and the Schiff base of DHA (dehydroacetic acid)⁵ can complex numerous metallic ions or difluoroboron moiety.^{6–8} In addition, the condensation of two hydrazino-TTF to a diketone was also studied with the aim of forming TTF dimers bearing a 1,4-(N,N) chelating group (molecules **D**, Fig. 2). In this paper we report on the synthesis of several bidentate electroactive ligands containing either one (**B**, **C**) or two TTF skeletons (**D**). The electrochemical characterizations of all these ligands as well as the structural properties are discussed. Preliminary complexation studies of dimer **D** towards molybdenum tetracarbonyl fragment and the synthesis of difluoroboron complexes of molecules **C** are also presented together with the influence of the complexation on the redox properties of the TTF.

* Corresponding author. Fax: +33 2 23 23 67 38; e-mail address: dominique.lorcy@univ-rennes1.fr (D. Lorcy).

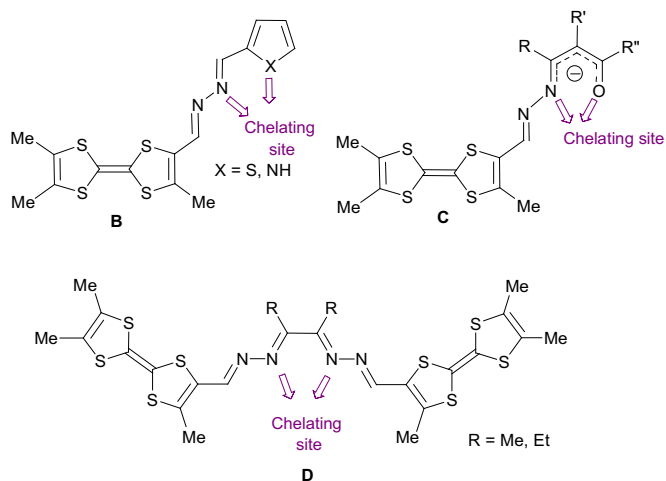


Fig. 2. Molecular structures of TTF-based ligands B, C and D.

2. Results and discussion

2.1. Synthesis and characterization of the ligands

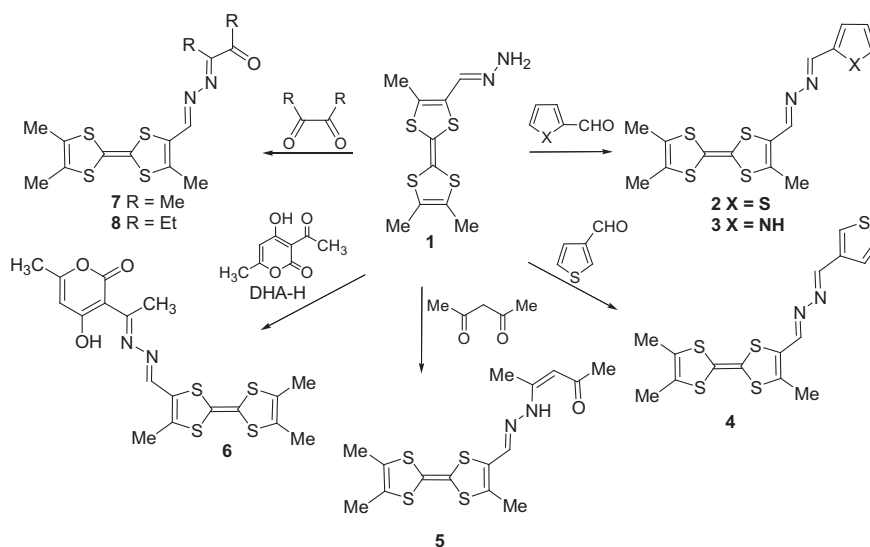
The condensation of Me₃-TTF hydrazone **1** with 2- and 3-thiophene carboxaldehyde and 2-pyrrole carboxaldehyde in THF at 50 °C affords TTF ligands **2**, **3** and **4**, respectively, as shown in Scheme 1. Both TTF **2** and **3** can be considered as potential (N,S) or (N,N) 1,4-bidentate ligands, which can behave as chelating ligands. With the aim of the grafting a β-enaminoketone part on the TTF through the azino linker, we also investigated the reaction of TTF hydrazone **1** with 1 equiv of acetylacetone in refluxing CH₃CN. Using this approach, TTF **5** was isolated in 80% yield. Similarly, the condensation reaction of the TTF hydrazone **1** with DHA–H in refluxing CH₃CN gives rise to a Schiff base of DHA connected to the TTF core through an azino linker, TTF **6**. These three derivatives, TTF **4**, **5** and **6**, can be evaluated as 1,5-bidentate ligands. However, TTF **4**, due to β-substitution of the thiophene ring, should not be able to chelate a metal center. In contrast, TTF **5** and **6**, treated in basic medium, would lead to the corresponding β-enaminoketonato ligands well known as efficient chelating systems.^{4–8} Another pathway to bidentate but neutral (N,O) ligand as **7** or **8** consists in

the reaction of TTF hydrazone **1** with diketones, such as butane-2,3-dione and hexane-3,4-dione as outlined in Scheme 1. The reaction of TTF **1** with an excess of the appropriate diketone in refluxing MeOH leads to TTF **7** (R=Me) and **8** (Et) in 40% and 61% yield, respectively.

Crystals suitable for an X-ray diffraction study have been obtained for TTF **3**, **4**, **5** and **8**, and their molecular structures are shown in Fig. 3. TTFs **3** and **4** exhibit similar overall flat geometry, with a planar TTF core and the five membered heterocycle practically coplanar. Concerning the linker between the TTF and the heterocycle, it can be observed also that the azino bridge are in an *anti* configuration and that the C9–C10 and C13–C14 bonds exhibit a similar conformation as they are all of *s-trans* type showing that TTF **3** could be the precursor of a potential chelating ligand.

The geometry of TTF **5** is slightly different as the TTF core is distorted and adopts a 'boat' structure as often observed with neutral TTF. The dithiole rings are folded along the S⋯S axis with an angle of about 13°. The bond lengths of the TTF core are those expected for a neutral TTF with a central C=C, which amounts to 1.349(9) Å. Concerning the linker between the ligand and the TTF in **5**, analysis of the bond lengths confirms that the linker is not anymore an azino structure but a hydrazone one due to the formation of the β-enaminoketone moiety with an *anti* configuration along the C10=N11 bond. This C10=N11 bond length within the hydrazone linker in **5** is similar to that in the azino linker in **3**, **4** while the C13–N12 bond length is longer in **5** compared to **3** and **4**. The bond lengths within the β-enaminoketone moiety are consistent with previous observations for β-enaminoketones⁹ and confirm the formation of the enaminoketone structure instead of the tautomeric forms, which could be also envisaged, such as the enolimine one or the ketoimine one as shown in Scheme 2.

The C=O (1.253(7) Å) and the C=C (1.295(7) Å) bond lengths are slightly longer than expected for pure C=O and C=C bonds while the C–C (1.434(8) Å) and the C–N (1.355(9) Å) are slightly shorter than expected. Moreover, the β-enaminoketone moiety is planar even with the presence of an sp³ nitrogen atom. This tends to indicate an electronic delocalization along the structure with the establishment of hydrogen bonding between the N and the O atoms as indeed observed with N–H⋯O1 [1.954(11) Å]. Concerning the molecular structure of TTF **8**, the azinopropanone moiety and the TTF core are coplanar. The TTF core itself is almost planar as the dithiole rings are folded along the S⋯S axis with an angle of 1 and



Scheme 1.

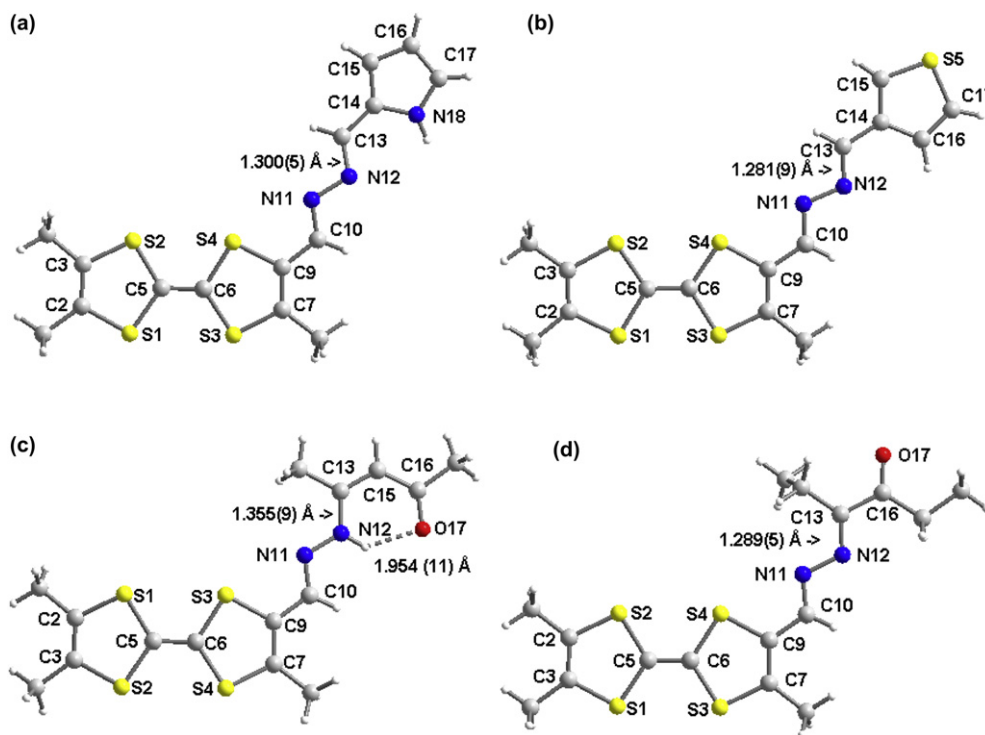
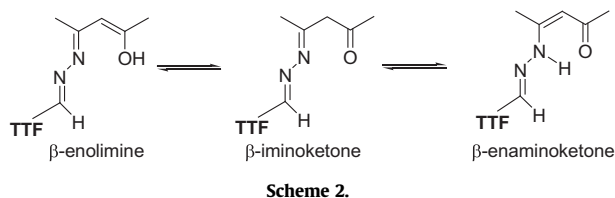


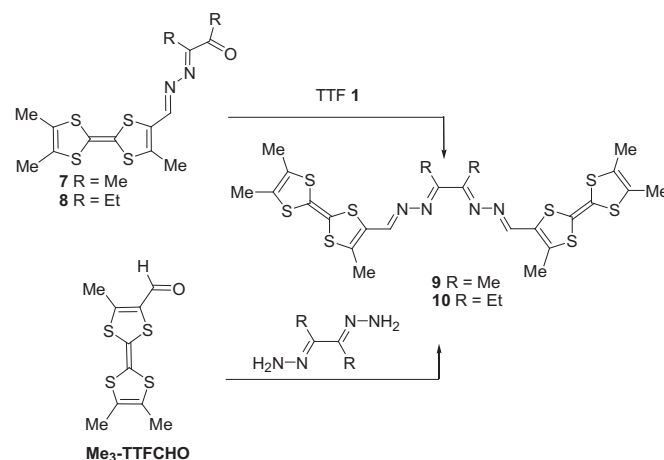
Fig. 3. Molecular structures of TTFs **3** (a), **4** (b), **5** (c) and **8** (d).



4°. The central C=C bond length of the TTF amounts to 1.346(6) Å and is characteristic for a neutral TTF. As previously observed for TTF **3** and **4**, the azino linker exhibit an *anti* configuration and the N=C bond and the C=O bond are in a *s-trans* configuration. This TTF exhibits two coordinating sites the oxygen and the nitrogen atoms, therefore it could behave as a (N,O)1,4-bidentate chelating ligand.¹⁰

The use of diketones in the condensation reaction with the hydrazone **1** would also allow the formation of TTF dimers connected through two azino bridges, which would also provide a chelating character to these electroactive ligands. Using α -diketones it is possible to build 1,4-bidentate ligand, with a bisazino moiety. In order to build these dimers, the first approach we used consists in reacting TTF **7** and **8** with 1 equiv of TTF **1** in refluxing MeOH for **9** and in refluxing CH₂Cl₂ for **10**. According to this strategy the overall yield starting from TTF carboxaldehyde was 17% and 9% for the symmetrical dimers **9** and **10**, respectively. We also investigated another route for the synthesis of these dimers by simply refluxing TTF carboxaldehyde with the bishydrazone of the diketone.¹¹ According to this second strategy (Scheme 3), the overall yield of the 1,4-bidentate ligands is increased to 49% for **9** and 66% for **10**. TTF **9** is poorly soluble in common organic solvents while the presence of the ethyl groups in **10** slightly increases the solubility.

Electrochemical investigations carried out by cyclic voltammetry show that all molecules containing one TTF core **2–8** display two reversible monoelectronic processes corresponding to the reversible oxidation of the TTF to the cation radical species and to



the dicationic one. The oxidation potentials are collected in Table 1 together with the oxidation potentials of the TTF precursor **1**. The substituent grafted on the azino linker exerts an electron withdrawing effect and decreases the electronic density on the TTF as both oxidation potentials are shifted to higher values compared to **1**. Concerning the TTF dimers **9** and **10** the first process is fully reversible and corresponds to the concomitant oxidation of both neutral TTF into the cation radical species while the second process is not fully reversible due to adsorption phenomena on the electrode. This second oxidation process corresponds to the oxidation of both radical cations into TTF dication. As both TTF oxidize simultaneously within these dimers, no interactions are detected electrochemically through the bisazino linker. Actually, this result is not surprising as within TTF dimers synthesized in the literature and connected through one conjugated spacer group, such as an ethylenic or an acetylenic linker, no splitting of the oxidation processes was observed.¹²

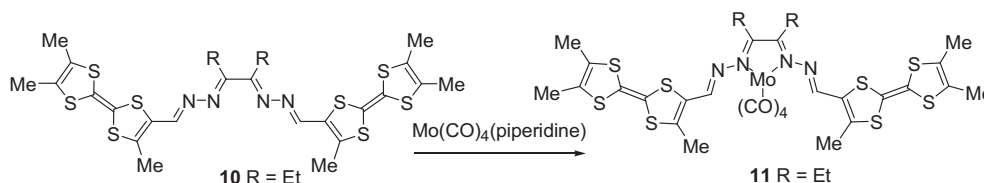
Table 1

Oxidation potentials of the TTFs **1**–**10**, E in V versus SCE, CH_2Cl_2 , Pt working electrode with 0.1 M $n\text{-Bu}_4\text{NPF}_6$ scanning rate 100 mV/s

Compound	E^1	E^2	ΔE mV
1	0.29	0.80	510
2	0.36	0.88	520
3	0.36	0.88	520
4	0.38	0.90	520
5	0.38	0.87	490
6	0.38	0.87	490
7	0.41	0.93	520
8	0.40	0.91	510
9	0.39	0.97/0.81	
10	0.40	0.97/0.80	

2.2. Molybdenum carbonyl complex

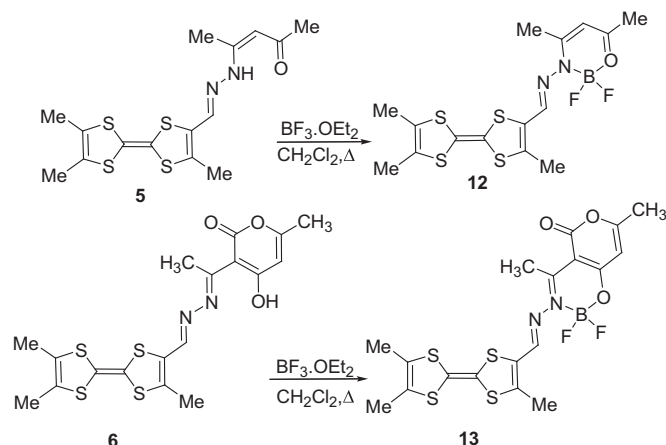
We have recently reported the formation of metal carbonyl complexes with TTF bearing an azinopyridine moiety and shown that the molybdenum is chelated by two nitrogen atoms: one from the azino linker and one from the pyridine.³ This result prompted us to investigate the reactivity of the TTF with two azino linkers, such as **10** towards $\text{cis-Mo}(\text{CO})_4(\text{piperidine})_2$. A solution of TTF **10** in CH_2Cl_2 in the presence of 1 equiv of $\text{cis-Mo}(\text{CO})_4(\text{piperidine})_2$ was stirred at room temperature for 1 h (Scheme 4). After purification by chromatography on silica gel column, a complex was isolated and analyzed by ^1H NMR spectroscopy. The ^1H NMR spectrum reveals that the signals observed for Et group, of the $-\text{N}=\text{CR}-\text{CR}=\text{N}-$ subunit, are slightly deshielded in the complex formed, when compared to the starting ligand. Similarly, the signal for the $\text{H}-\text{C}=\text{N}$ resonates at a lower field in complex **11** than in ligand **10**. These chemical shifts are coherent with the coordination of the electroactive ligand **10** to the molybdenum atom. Moreover, only one signal is observed for this proton which implies a similar environment and presumably the chelation of a $\text{Mo}(\text{CO})_4$ fragment.

**Scheme 4.**

IR spectroscopy gave us confirmation about the nature of the $\text{Mo}(\text{CO})_n$ fragment coordinated to the $-\text{N}=\text{CR}-\text{CR}=\text{N}-$. Indeed, specific vibrations can be observed depending on the number of remaining carbonyl groups. On the spectrum of **11**, in the carbonyl region, stretching absorption bands were observed at 2012, 1921, 1881, 1845 cm^{-1} characteristic for a $\text{Mo}(\text{CO})_4$ ¹³ fragment, which implies that the molybdenum is chelated by the electroactive ligand in order to form $[\text{Mo}(\text{CO})_4(\text{TTF-N,N,N,N-TTF})]$ **11**.

2.3. Difluoroboron β -enaminoketonato complexes

In order to prepare the TTF functionalized by a β -enaminoketonato complex of difluoroboron, we added an excess of boron trifluoride diethyl etherate ($\text{BF}_3 \cdot \text{OEt}_2$) in the presence of triethylamine to a solution of TTF **5** and **6** in dichloromethane under inert atmosphere. The target complexes **12** and **13** are obtained as air stable derivatives after purification by column chromatography on silica gel (Scheme 5). ^1H NMR spectra of both derivatives show some noticeable downfield shifts of the protons close to the boron–enaminoketonato ring. For instance, H_{15} and H_{10} originally observed, respectively, at 5.14 and 7.75 ppm in ligand **5** are shifted to 5.43 and 8.66 ppm in complex **12**. ^{11}B and ^{19}F NMR investigations

**Scheme 5.**

in solution are a convenient tool for structural symmetry determination of the 1,3-enaminoketonatoboron difluorides ring.⁶ In both cases, ^{11}B NMR spectra of **12** and **13** exhibit one triplet close to 0 ppm due to the coupling of the boron atom with two magnetically equivalent fluorine atoms. In the ^{19}F NMR spectra the fluorine atoms resonate at -113.4 and -136.4 ppm for **12** and **13**, respectively, four line signals appear for these nuclei due to the coupling with the boron atom ($I=3/2$, ^{11}B).¹⁴

In order to study the influence of the BF_2 moiety on the donating ability of the TTF core, we performed electrochemical investigations. Two reversible mono-electronic oxidation waves are observed for derivatives **12** and **13**. Compared with the starting ligand, **5** and **6**, the oxidation potentials are shifted towards more positive potentials indicating the electron withdrawing effect of the 1,3-enaminoketonatoboron difluorides ring on the TTF core (Table 2) It is worth-

noting that on cathodic scan no reduction process was observed as in the case of other difluoroboron complexes of ketoinimato.⁶ Actually, this was already the case with acetylacetonate analogues, such as TTF acetylacetonate complexes of difluoroboron.¹⁵ According to literature, the reduction process is close to -1.8 V versus Ag/AgCl and therefore the presence of the TTF, an electron rich substituent, might induces a shift of the reduction outside the potential window.

Table 2

Oxidation potentials of the TTFs **11**–**14**, E in V versus SCE, CH_2Cl_2 0.1 M, Pt working electrode with 0.1 M $n\text{-Bu}_4\text{NPF}_6$ scanning rate 100 mV/s

Compound	E^1	E^2	ΔE mV
11	0.38	0.90	520
12 (5)	0.42 (0.38)	0.93 (0.87)	510 (490)
13 (6)	0.43 (0.38)	0.94 (0.87)	510 (490)

Crystals have been obtained after recrystallization of **12** in toluene. The molecular structure of **12** is shown in Fig. 4 and it is interesting to note that the molecular shape of **12** is very similar to the starting ligand **5** concerning the configuration of the azino linker between the TTF and the chelate ring. However some differences can be noticed, such as a planar core for the TTF and some

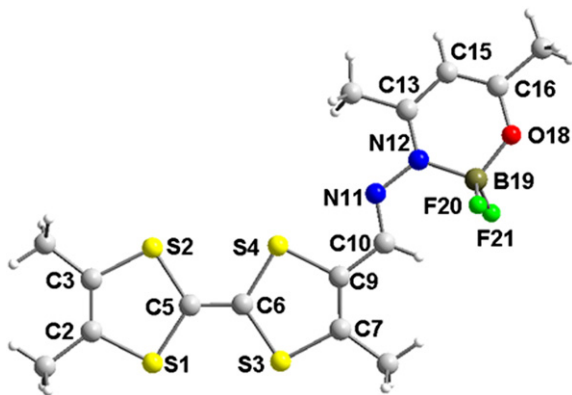
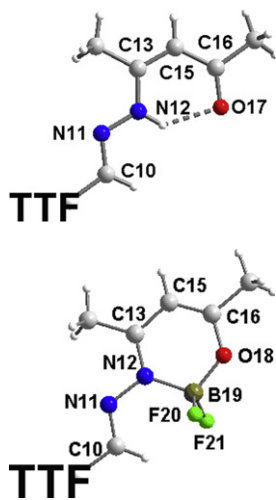


Fig. 4. Molecular structure of **12**.

bond lengths modification especially on the chelate ring. In Table 3, we collected selected bond lengths and angles of the chelate ring in **12** together with those of the starting ligand **5**. Comparison of the bond lengths indicates that both structures exhibit a delocalized π -electron system with a different electron distribution. Indeed, within complex **12**, compared to **5**, the C–N bond is shortened (ca. 0.03 Å) while the C–O bond is lengthened (ca. 0.06 Å) indicating an enolate–imine contribution of the chelate ring in **12**. This differs from what was observed for **5** as, in the solid state, the bond lengths are in accordance with a ketoamine distribution. Both chelate rings are planar with similar bond angles but due to the presence of the difluoroboron moiety in **12** and therefore to steric strain the bond angles of the linker are different.

Table 3
Comparison of selected bond lengths in Å and angles in ° of the chelate ring in TTFs **5** and **12**



Bond lengths	TTF 5	TTF 12	Bond angles	TTF 5	TTF 12
C10–N11	1.295(7)	1.293(2)	C9–C10–N11	119.44(15)	116.75(15)
N11–N12	1.374(8)	1.403(3)	C10–N11–N12	114.63(15)	117.90(15)
N12–C13	1.355(9)	1.327(3)	N11–N12–C13	121.14(15)	114.38(16)
C13–C15	1.380(8)	1.411(3)	N11–C13–C15	119.79(17)	119.41(19)
C15–C16	1.434(8)	1.360(4)	C13–C15–C16	123.77(18)	121.97(20)
C16–O	1.253(7)	1.318(3)	C15–C16–O	123.13(21)	121.27(22)
C5–C6	1.349(9)	1.354(3)			

3. Conclusions

A series of bidentate redox active ligands containing either one or two TTFs cores have been synthesized readily thanks to the

ability of TTF hydrazone, an efficient precursor, to condense with various carbonyl derivatives. As evidenced by the X-ray diffraction studies, these derivatives are almost planar with either the 1,4- or 1,5-chelating sites in the plane of the TTF. We also investigated their electrochemical properties and demonstrated that these redox active ligands exhibit easily accessible oxidation states leading to promising ligands for further metal coordination. To illustrate their chelating ability, we prepared molybdenum tetracarbonyl complex and difluoroboron complexes and confirmed the non innocent character of the azino linker. These results open great potential for the elaboration of both low valent and high valent metal complexes as it is possible to modulate the number of electron brought by the chelating motifs (X_2 , LX , L_2 ligands) depending on the nature of the carbonyl derivatives condensed to TTF hydrazone.

4. Experimental

4.1. General

^1H NMR, ^{13}C NMR, ^{11}B NMR and ^{19}F NMR spectra were recorded on a Bruker Avance 300 III spectrometer with tetramethylsilane as internal reference using CDCl_3 as solvent unless otherwise stated. Chemical shifts are reported in parts per million. Mass spectra and elemental analysis results were performed by the Centre de Mesures Physiques de l'Ouest, Rennes. Melting points were measured using a Kofler hot stage apparatus and are uncorrected. Cyclic voltammetry were carried out on a 10^{-3} M solution of the compounds in dichloromethane, containing 0.1 M $n\text{-Bu}_4\text{NPF}_6$ as supporting electrolyte. Voltammograms were recorded at 0.1 Vs^{-1} on a platinum disk electrode ($A=1 \text{ mm}^2$). The potentials were measured versus Saturated Calomel Electrode. *cis*- $\text{Mo}(\text{CO})_4(\text{NC}_5\text{H}_{11})_2$ was prepared according to published procedure.¹⁶ All the reagents were purchased and used without additional purification.

4.2. Synthesis and characterization

4.2.1. General procedure for the synthesis of TTF (2–4). To a solution of TTF **1** (0.144 g, 0.5 mmol) in 30 mL of THF was added 0.55 mmol of the aldehyde (62 mg for 2-thiophenecarboxaldehyde or 3-thiophene carboxaldehyde and 52 mg for pyrrole-2-carboxaldehyde). The resulting solution was stirred at 50°C for 3 h. The solvent was evaporated and the residue was chromatographed on silica gel column using CH_2Cl_2 as eluent. The precipitate was recrystallized in $\text{EtOH}/\text{CH}_2\text{Cl}_2$ (1/1).

TTF **2** was obtained as brown powder in 57% yield. $\text{Mp}=208^\circ\text{C}$; ^1H NMR δ 1.96 (s, 6H, CH_3), 2.27 (s, 3H, CH_3), 7.12 (m, 1H, CH), 7.43 (m, 1H, CH), 7.49 (m, 1H, CH), 8.48 (s, 1H, CH), 8.75 (s, 1H, CH); ^{13}C NMR δ 13.7, 13.8, 14.3, 105.7, 111.6, 122.5, 123.1, 126.9, 127.9, 130.2, 132.7, 138.8, 142.0, 151.7, 156.3; UV–vis (CH_2Cl_2) λ (nm) ($\epsilon \text{ L mol}^{-1} \text{ cm}^{-1}$): 284 (17,100), 336 (37,700), 500 (6800); IR (cm^{-1}) 1604 ν (C=N–); HRMS calcd for $\text{C}_{15}\text{H}_{14}\text{N}_2\text{S}_5 \text{ M}^+$ 381.9755. Found 381.9756.

TTF **3** was obtained in 49% yield as orange crystals. $\text{Mp}=191^\circ\text{C}$; ^1H NMR δ 1.97 (s, 6H, CH_3), 2.25 (s, 3H, CH_3), 6.32 (m, 1H, CH), 6.66 (m, 1H, CH), 7.01 (m, 1H, CH), 8.40 (s, 1H, CH), 8.42 (s, 1H, CH), 9.32 (br,s, 1H, NH); ^{13}C NMR δ 13.7, 13.8, 14.3, 105.9, 110.8, 111.4, 117.1, 122.5, 122.9, 123.1, 127.0, 127.5, 140.3, 150.0, 152.7; UV–vis (CH_2Cl_2) λ (nm) ($\epsilon \text{ L mol}^{-1} \text{ cm}^{-1}$) 346 (36,650), 467 (5800); IR (cm^{-1}): 1608 ν (C=N–); HRMS calcd for $\text{C}_{15}\text{H}_{15}\text{N}_3\text{S}_4 \text{ M}^+$ 365.0143. Found 365.0142; Anal. Calcd for $\text{C}_{15}\text{H}_{15}\text{N}_3\text{S}_4$: C, 49.28; H, 4.14; N, 11.49. Found C, 48.71; H, 4.22; N, 11.38.

TTF **4** was obtained in 52% yield as orange crystals. $\text{Mp}=193^\circ\text{C}$; ^1H NMR δ 1.97 (s, 6H, CH_3), 2.28 (s, 3H, CH_3), 7.38 (m, 1H, CH), 7.58 (m, 1H, CH), 7.73 (m, 1H, CH), 8.50 (s, 1H, CH), 8.63 (s, 1H, CH); ^{13}C NMR δ 13.7, 13.8, 14.3, 105.7, 111.6, 122.5, 123.1, 125.6, 126.8, 130.1, 137.4, 141.7, 151.7, 157.2; UV–vis (CH_2Cl_2) λ (nm) ($\epsilon \text{ L mol}^{-1} \text{ cm}^{-1}$) 318 (43,600), 481 (5860); IR

(cm^{-1})=1615 $\nu(\text{C}=\text{N}-)$; HRMS calcd for $\text{C}_{15}\text{H}_{14}\text{N}_2\text{S}_5 \text{M}^+$: 381.97551. Found 381.9756; Anal. Calcd for $\text{C}_{15}\text{H}_{14}\text{N}_2\text{S}_5$: C, 47.09; H, 3.69; N, 7.32. Found: C, 47.06; H, 3.72; N, 7.22.

4.2.2. General procedure for the synthesis of TTF (5–8). To a solution of TTF **1** (200 mg, 0.7 mmol) in CH_3CN 20 mL (for **5** and **6**) or MeOH 20 mL (for **7** and **8**) was added 0.75 mmol of either the diketone (acetylacetone 75 mg for the synthesis of **5**, DHA–H 126 mg for the synthesis of **6**, 2,3-butanedione 65 mg for the synthesis of **7**, 3,4-hexane-dione 85 mg for the synthesis of **8**). The reaction mixture was refluxed for 4 h. The solvent was removed under vacuum and the precipitate was subject to column chromatography using CH_2Cl_2 as eluent.

TTF **5** was obtained as brown powder in 80% yield. Mp=207 °C; ^1H NMR (CDCl_3 , 300 MHz) δ =1.95 (s, 6H, CH_3), 2.08 (s, 3H, CH_3), 2.15 (s, 3H, CH_3), 2.17 (s, 3H, CH_3), 5.14 (s, 1H, CH), 7.75 (s, 1H, CH), 13.42 (s, 1H, OH); ^{13}C NMR (CDCl_3 , 75 MHz) δ 13.6, 13.7, 14.1, 18.2, 29.2, 96.4, 106.1, 110.8, 122.7, 122.9126.4, 135.3, 135.9, 159.3, 196.8; UV–vis (CH_2Cl_2) λ (nm) (ϵ L mol $^{-1}$ cm $^{-1}$) 295 (10,370), 367 (21,360), 447 (6920); IR (cm^{-1}): 1616 $\nu(\text{C}=\text{O})$, 1575 $\nu(\text{C}=\text{N})$; HRMS calcd for $\text{C}_{15}\text{H}_{18}\text{N}_2\text{OS}_4$ 370.0296. Found 370.0293.

DHA-azino-TTF **6**. The product was purified by column chromatography using $\text{CH}_2\text{Cl}_2/\text{MeOH}$ (9.8/0.2) as eluent. TTF **6** was obtained as a dark purple powder in 59% yield. Mp=274 °C; ^1H NMR δ 1.96 (s, 6H, CH_3), 2.17 (s, 3H, CH_3), 2.26 (s, 3H, CH_3), 2.88 (s, 3H, CH_3), 5.74 (s, 1H, CH), 8.09 (s, 1H, CH=N); ^{13}C NMR (CDCl_3) δ 12.7, 12.7, 13.4, 16.0, 18.9, 95.1, 105.8, 112.1, 121.7, 122.1, 142.6, 142.8, 142.9, 162.0, 162.7, 171.6, 183.6; IR (cm^{-1}): 1590 $\nu(\text{C}=\text{N})$, 1616 $\nu(\text{C}=\text{O})$; UV–vis (CH_2Cl_2) λ (nm) (ϵ L mol $^{-1}$ cm $^{-1}$): 369 (34,400), 383 (36,300), 525 (6600); HRMS calcd for $\text{C}_{18}\text{H}_{18}\text{N}_2\text{O}_3\text{S}_4$ 438.0200. Found 438.0194.

TTF **7** was obtained in 40% yield as a dark red powder. Mp 168 °C; ^1H NMR δ 1.94 (s, 6H, CH_3), 2.08 (s, 3H, CH_3), 2.27 (s, 3H, CH_3), 2.45 (s, 3H, CH_3), 8.17 (s, 1H, CH); ^{13}C NMR δ 10.7, 12.7, 12.8, 13.4, 24.0, 104.2, 111.0, 121.6, 122.1, 126.6, 142.7, 148.0, 162.5; IR (cm^{-1}): 1686 $\nu(\text{C}=\text{O})$, 1598 $\nu(\text{C}=\text{N})$, 1547 $\nu(\text{C}=\text{N})$; UV–vis (CH_2Cl_2) λ (nm) (ϵ L mol $^{-1}$ cm $^{-1}$) 286 (18,580), 315 (21,680), 511 (3620); HRMS calcd for $\text{C}_{14}\text{H}_{16}\text{N}_2\text{OS}_4$: 356.0140. Found: 356.0139.

TTF **8** was obtained as a dark red solid in 61% yield. Mp 163 °C; ^1H NMR δ 1.02 (t, 3H), 1.12 (t, 3H), 1.96 (s, 6H, CH_3), 2.28 (s, 3H, CH_3), 2.67 (q, 2H, CH_2), 2.91 (q, 2H, CH_2), 8.19 (s, 1H, CH); ^{13}C NMR (CDCl_3): 8.0, 11.3, 13.7, 14.4, 19.3, 22.3, 30.7, 105.4, 111.8, 122.6, 123.1, 127.7, 143.2, 149.1, 167.7; IR (cm^{-1}): 1686 $\nu(\text{C}=\text{O})$, 1574 $\nu(\text{C}=\text{N})$, 1535 $\nu(\text{C}=\text{N})$; UV–vis (CH_2Cl_2) λ (nm) (ϵ L mol $^{-1}$ cm $^{-1}$) 278 (33,190), 317 (42,800), 509 (7120); HRMS calcd for $\text{C}_{16}\text{H}_{20}\text{N}_2\text{OS}_4$: 384.0453. Found: 384.0448.

4.2.3. Synthesis of dimers TTF (9) and (10) starting from TTF (7) and (8). To a solution of TTF **1** (0.24 mmol, 68 mg) in 20 mL of MeOH was added TTF **6** (0.24 mmol, 84 mg). The reaction mixture was refluxed for 12 h. After cooling the reaction mixture to room temperature, a dark precipitate was filtered off, washed with MeOH to afford dimer **9** as poorly soluble deep purple powder in 85% yield (overall yield for **9** using this two step procedures 17% starting from TTF carboxaldehyde). Mp >260 °C; ^1H NMR δ 1.27 (s, 6H, CH_3), 1.97 (s, 12H, CH_3), 2.32 (s, 6H, CH_3), 8.22 (s, 2H, CH=N); IR (cm^{-1}): 1590 $\nu(\text{C}=\text{N})$; UV–vis (CH_2Cl_2) λ (nm) (ϵ L mol $^{-1}$ cm $^{-1}$): 285 (23,080), 330 (32,620), 522 (6620); HRMS calcd for $\text{C}_{24}\text{H}_{26}\text{N}_4\text{S}_8$ 625.9917. Found 625.9923.

Similar procedure was used for the synthesis of dimer **10** using CH_2Cl_2 instead of MeOH. TTF **10** was obtained, after a chromatography on silica gel column using CH_2Cl_2 as eluent, as deep purple powder in 30% yield (overall yield for **10** using this procedures 9% starting from TTF carboxaldehyde). Mp=197 °C; ^1H NMR δ 1.05 (t, 6H, CH_3), 1.96 (s, 12H, CH_3), 2.27 (s, 6H, CH_3), 2.89 (q, 4H, CH_2), 8.21 (s, 2H, CH=N); IR (cm^{-1}): 1590 $\nu(\text{C}=\text{N})$; UV–vis (CH_2Cl_2) λ (nm)

(ϵ L mol $^{-1}$ cm $^{-1}$): 285 (14,560), 330 (20,100), 525 (4330); HRMS calcd for $[\text{M}+\text{Na}]^+$ $\text{C}_{26}\text{H}_{30}\text{N}_4\text{NaS}_8$ 677.0128. Found 677.0130.

4.2.4. Synthesis of dimers TTF (9) and (10) starting from Me₃TTF-carboxaldehyde. For TTF **9**: a suspension of Me₃TTF-carboxaldehyde (550 mg, 2 mmol) and 2,3-butadihydrazone (1 mmol, 114 mg) in 50 mL of MeOH was heated to reflux overnight. After cooling the reaction mixture to room temperature, a dark precipitate was filtered off, washed with MeOH to afford dimer **9** as poorly soluble deep purple powder in 49% yield.

For TTF **10**: a solution of Me₃TTF-carboxaldehyde (550 mg, 2 mmol) and 3,4-hexanedihydrazone (1 mmol, 140 mg) in 30 mL of CH_2Cl_2 was heated to reflux overnight and then the solvent was removed in vacuo. The product was purified by column chromatography using CH_2Cl_2 as eluent. TTF dimer **10** was obtained in 66% yield.

4.2.5. Synthesis of cis-Mo(CO)₄(TTF-N,N,N-TTF) (11). To a solution of TTF **10** (70 mg, 0.076 mmol) in 15 ml of dried, degassed CH_2Cl_2 was added under argon cis-Mo(CO)₄(C₅H₁₀NH)₂ (26 mg, 0.076 mmol). The reaction mixture was stirred for 4 h under reflux and then allowed to reach room temperature. The precipitate was filtered off and purified by column chromatography using CH_2Cl_2 as eluent (R_f 0.95). The complex **11** was obtained as a deep blue powder in 25% yield. Mp >260 °C; ^1H NMR 1.19 (t, 6H, CH_3), 1.98 (s, 12H, CH_3), 2.44 (s, 6H, CH_3), 2.95 (m, 4H, CH_2), 9.15 (s, 2H, CH=N); IR (cm^{-1}): 2012 $\nu(\text{CO})$, 1921 $\nu(\text{CO})$, 1881 $\nu(\text{CO})$, 1845 $\nu(\text{CO})$, 1558 $\nu(\text{C}=\text{N})$; HRMS calcd for $\text{C}_{30}\text{H}_{30}\text{N}_4\text{O}_4\text{S}_8\text{Mo}$: 857.9101. Found: 857.9088

4.2.6. Synthesis of difluoroboron complexes (12) and (13). An excess of $\text{BF}_3 \cdot \text{OEt}_2$ (0.7 mL, 5 mmol) was added to a solution of TTF **5** (185 mg for **5** and 220 mg for **6**, 0.5 mmol) and NET_3 (250 mg, 1.5 mmol) in 20 mL of dry and degassed CH_2Cl_2 under inert atmosphere. The reaction mixture was stirred at room temperature for 5 h. The organic phase was washed with water 3×20 mL, dried over MgSO_4 . The TTFs **12** and **13** were obtained after column chromatography using CH_2Cl_2 as eluent.

TTF (**12**), deep purple powder, 15% yield. Mp >260 °C; ^1H NMR (300 MHz) δ 1.95 (s, 6H, CH_3), 2.16 (s, 3H, CH_3), 2.29 (s, 3H, CH_3), 2.35 (s, 3H, CH_3), 5.43 (s, 1H, CH), 8.66 (s, 1H, CH); ^{13}C NMR (75 MHz) δ 13; 7, 14.6, 19.9, 22.7, 98.3, 111.7, 122.8, 122.9, 127.5, 146.5, 146.6, 169.7, 175.8; ^{11}B NMR (96 MHz) δ 0.69 (t, $J_{\text{B-F}}=16.8$ Hz); ^{19}F (282 MHz) δ -133.4 (q, $J_{\text{B-F}}=16.8$ Hz); UV–vis (CH_2Cl_2) λ (nm) (ϵ L mol $^{-1}$ cm $^{-1}$): 293 (11,900), 355 (25,700), 515 (4830); IR (cm^{-1}): 1575 $\nu(\text{C}=\text{N})$; Anal. Calcd for $\text{C}_{15}\text{H}_{17}\text{BF}_2\text{N}_2\text{OS}_4$: C, 43.06; H, 4.10. Found: C, 43.02; H, 4.09.

TTF (**13**) 23% yield. Mp >260 °C; ^1H NMR (300 MHz): 1.96 (s, 6H, CH_3), 2.33 (s, 6H, CH_3), 2.92 (s, 3H, CH_3), 6.06 (s, 1H, CH), 8.65 (s, 1H, CH); ^{11}B NMR (96 MHz) δ -0.14 (t, $J_{\text{B-F}}=16$ Hz); ^{19}F (282 MHz) δ -136.4 (q, $J_{\text{B-F}}=16$ Hz); UV–vis (CH_2Cl_2) λ (nm) (ϵ L mol $^{-1}$ cm $^{-1}$): 369 (34,080), 558 (6670); HRMS calcd for $\text{C}_{18}\text{H}_{17}\text{BF}_2\text{N}_2\text{O}_3\text{S}_4$: 486.01832. Found: 486.0184

4.3. Crystallography

Single-crystal diffraction data were collected on APEX II Bruker AXS diffractometer, Mo $K\alpha$ radiation ($\lambda=0.71073$ Å), for compounds **3**, **4**, **5**, **8** and **12** (Centre de Diffraction X, Université de Rennes, France). The structures were solved by direct methods using the SIR97 program,¹⁷ and then refined with full-matrix least-square methods based on F^2 (SHELX-97)¹⁸ with the aid of the WINGX program.¹⁹ All non-hydrogen atoms were refined with anisotropic displacement parameters. H atoms were finally included in their calculated positions.

Crystal data for **3**: ($\text{C}_{15}\text{H}_{15}\text{N}_3\text{S}_4$); $M=365.54$. $T=100(2)$ K; orthorhombic P bna , $a=8.0663(6)$, $b=9.5104(7)$, $c=42.281(3)$ Å,

$V=3243.5(4) \text{ \AA}^3$, $Z=8$, $d=1.497 \text{ g cm}^{-3}$, $\mu=0.584 \text{ mm}^{-1}$. A final refinement on F^2 with 3613 unique intensities and 202 parameters converged at $\omega R(F^2)=0.1043$ ($R(F)=0.0542$) for 1994 observed reflections with $I>2\sigma(I)$.

Crystal data for **4**: ($\text{C}_{15}\text{H}_{14}\text{N}_2\text{S}_5$); $M=382.58$. $T=100(2) \text{ K}$; monoclinic $P 2_1/a$, $a=7.4020(16)$, $b=9.813(2)$, $c=22.814(5) \text{ \AA}$, $\beta=90.600(7)^\circ$, $V=1657.0(6) \text{ \AA}^3$, $Z=4$, $d=1.534 \text{ g cm}^{-3}$, $\mu=0.695 \text{ mm}^{-1}$. A final refinement on F^2 with 3417 unique intensities and 203 parameters converged at $\omega R(F^2)=0.16$ ($R(F)=0.0716$) for 2447 observed reflections with $I>2\sigma(I)$.

Crystal data for **5**: ($\text{C}_{15}\text{H}_{18}\text{N}_2\text{OS}_4$); $M=370.55$. $T=150(2) \text{ K}$; triclinic $P-1$, $a=7.8062(16)$, $b=8.1019(17)$, $c=14.462(3) \text{ \AA}$, $\alpha=74.429(9)$, $\beta=82.231(10)$, $\gamma=87.287(11)^\circ$, $V=872.9(3) \text{ \AA}^3$, $Z=2$, $d=1.41 \text{ g cm}^{-3}$, $\mu=0.546 \text{ mm}^{-1}$. A final refinement on F^2 with 3812 unique intensities and 204 parameters converged at $\omega R(F^2)=0.0775$ ($R(F)=0.0324$) for 3068 observed reflections with $I>2\sigma(I)$.

Crystal data for **8**: ($\text{C}_{16}\text{H}_{20}\text{N}_2\text{OS}_4$); $M=384.58$. $T=150(2) \text{ K}$; triclinic $P-1$, $a=7.5901(11)$, $b=7.5989(11)$, $c=16.580(2) \text{ \AA}$, $\alpha=87.004(6)$, $\beta=89.453(7)$, $\gamma=77.050(6)^\circ$, $V=930.7(2) \text{ \AA}^3$, $Z=2$, $d=1.372 \text{ g cm}^{-3}$, $\mu=0.515 \text{ mm}^{-1}$. A final refinement on F^2 with 4050 unique intensities and 213 parameters converged at $\omega R(F^2)=0.0936$ ($R(F)=0.038$) for 3018 observed reflections with $I>2\sigma(I)$.

Crystal data for **12**: ($2(\text{C}_{15}\text{H}_{17}\text{BF}_2\text{N}_2\text{OS}_4)$, C_7H_8); $M=928.85$. $T=150(2) \text{ K}$; triclinic $P-1$, $a=7.8540(6)$, $b=8.1202(6)$, $c=17.2584(12) \text{ \AA}$, $\alpha=93.218(2)$, $\beta=90.721(2)$, $\gamma=103.024(2)^\circ$, $V=1070.31(14) \text{ \AA}^3$, $Z=1$, $d=1.441 \text{ g cm}^{-3}$, $\mu=0.474 \text{ mm}^{-1}$. A final refinement on F^2 with 4670 unique intensities and 267 parameters converged at $\omega R(F^2)=0.0906$ ($R(F)=0.0364$) for 3751 observed reflections with $I>2\sigma(I)$.

5. Supplementary data

Crystallographic data for structural analysis have been deposited with the Cambridge Crystallographic Data Centre, CCDC No 812737–812741 for compounds **3**, **4**, **5**, **8** and **12**, respectively. Copies of this information may be obtained free of charge from The CCDC,

12 Union road, Cambridge CB2 1EZ, UK (fax: +44 1223 336033; e-mail: deposit@ccdc.cam.ac.uk or <http://www.ccdc.cam.ac.uk>).

References and notes

- Lorcy, D.; Bellec, N.; Fourmigué, M.; Avarvari, N. *Coord. Chem. Rev.* **2009**, *253*, 1398–1438.
- (a) Canevet, D.; Sallé, M.; Zhang, G.; Zhang, D.; Zhu, D. *Chem. Commun.* **2009**, 2245–2269; (b) Shatruck, M.; Ray, L. *Dalton Trans.* **2010**, 39, 11105–11121; (c) Rabaca, S.; Almeida, M. *Coord. Chem. Rev.* **2010**, *254*, 1493–1508.
- Bakhta, S.; Guerro, M.; Kolli, B.; Barrière, F.; Roisnel, T.; Lorcy, D. *Tetrahedron Lett.* **2010**, *51*, 4497–4500.
- Ye, W.-P.; Shi, X.-C.; Li, B.-X.; Liu, J.-Y.; Li, Y.-S.; Cheng, Y.-X.; Hu, N.-H. *Dalton Trans.* **2010**, 39, 9000–9007; Brown, J. L.; Wu, G.; Hayton, T. W. *J. Am. Chem. Soc.* **2010**, *132*, 7248–7249; Ye, W.-P.; Zhan, J.; Pan, L.; Hu, N.-H.; Li, Y.-S. *Organometallics* **2008**, *27*, 3642–3653; Wang, H.-Y.; Zhang, J.; Meng, X.; Jin, G.-X. *J. Organomet. Chem.* **2006**, *691*, 1275–1281; Richeter, S.; Jeandon, C.; Gisselbrecht, J.-P.; Graff, R.; Ruppert, R.; Callot, H. J. *Inorg. Chem.* **2004**, *43*, 251–263; Li, X.-F.; Dai, K.; Ye, W.-P.; Pan, L.; Li, Y.-S. *Organometallics* **2004**, *23*, 1223–1230; Roll, C. P.; Martin, A. G.; Goerls, H.; Leibel, G.; Guillon, D.; Donnio, B.; Wolfgang, W. *J. Mater. Chem.* **2004**, *14*, 1722–1730; He, X.-H.; Yao, Y.-Z.; Luo, X.; Zhang, J.-K.; Liu, Y.-H.; Zhang, L.; Wu, Q. *Organometallics* **2003**, *22*, 4952–4957.
- Kannan, S.; Ramesh, R. *Polyhedron* **2006**, *25*, 3095–3103.
- Macedo, F. P.; Gwengo, C.; Lindeman, S. V.; Smith, M. D.; Gardinier, J. R. *Eur. J. Inorg. Chem.* **2008**, 3200–3211.
- Xia, M.; Wu, B.; Xiang, G. *J. Fluorine Chem.* **2008**, *129*, 402–408.
- Itoh, K.; Fujimoto, M.; Hashimoto, M. *New J. Chem.* **2002**, *26*, 1070–1075.
- Xia, M.; Wu, B.; Xinag, G.-F. *Synth. Commun.* **2008**, *38*, 1268–1278.
- Lu, C. C.; Bill, E.; Weyhermüller, T.; Bothe, E.; Wieghardt, K. *Inorg. Chem.* **2005**, *46*, 7880–7889.
- Hauer, C. R.; King, G. S.; McCool, E. L.; Euler, W. B.; Ferrara, J. D.; Youngs, W. J. *J. Am. Chem. Soc.* **1987**, *109*, 5760–5765.
- (a) Iyoda, M.; Hasegawa, M.; Miyake, Y. *Chem. Rev.* **2004**, *104*, 5085–5113; (b) Otsubo, T.; Kochi, Y.; Bitoh, A.; Ogura, F. *Chem. Lett.* **1994**, 2047–2050; (c) Iyoda, M.; Hasegawa, M.; Takano, J. I.; Hara, K.; Kuwatani, Y. *Chem. Lett.* **2002**, 590–591.
- Kraihanzel, C. S.; Cotton, F. A. *Inorg. Chem.* **1963**, *2*, 533–540.
- Itoh, K.; Okazaki, K.; Fujimoto, M. *Aust. J. Chem.* **2003**, *56*, 1209–1214.
- Guerro, M.; Roisnel, T.; Lorcy, D. *Tetrahedron* **2009**, *65*, 6123–6127.
- Darensbourg, D.; Kump, R. L. *Inorg. Chem.* **1978**, *17*, 2680–2682.
- Altomare, A.; Burla, M. C.; Camalli, M.; Cascarano, G.; Giacovazzo, C.; Guagliardi, A.; Moliterni, A. G. G.; Polidori, G.; Spagna, R. *J. Appl. Crystallogr.* **1999**, *32*, 115–119.
- Sheldrick, G. M. *Acta Crystallogr.* **2008**, *A64*, 112–122.
- Farrugia, L. J. *J. Appl. Crystallogr.* **1999**, *32*, 837–838.